Lasers in Surgery and Medicine 20:280–289 (1997)

Laser Ablation of Dyed Acrylic Bone Cement

Chi L. Lee, MS,[1,2] Cynthia Roberts, PhD,[1*] and Alan S. Litsky, MD, ScD[1,2]

[1]Biomedical Engineering Center, The Ohio State University, Columbus, Ohio
[2]Orthopaedic BioMaterials Laboratory, The Ohio State University, Columbus, Ohio 43210-1069

Revision surgery of cemented implants is indicated when mechanical failure causes severe pain and/or loss of function for the patient. Successful revision arthroplasty of cemented implants requires complete removal of the existing cement. Removal of old cement is an arduous task often causing damage to the surrounding bone tissue. In this study, the authors investigate the use of an Argon laser and the addition of dyes to enhance the laser ablation of bone cement. Methylene blue and red dye #13 were each added separately to polymethylmethacrylate (PMMA) bone cement powder. A continuous wave Argon ion laser (λ = 514 nm) was used for cement ablation. Cement samples were ablated at different power levels (1.5, 2.3, and 3.0 W) and exposure times (30, 60, 90, 120 sec). The results show that the Argon laser was unable to ablate undyed PMMA. However, the addition of either methylene blue or red dye #13 greatly improved cement ablation by altering the cements' absorption characteristics. Results of Student's *t*-tests show a statistical difference between red and blue dyed PMMA mean ablation areas at all energy levels tested (P < .0002). As expected, all red ablation areas were greater than blue ablation areas at each energy level tested since red dye absorbs more energy at 514 nm than methylene blue dye. The results of this study suggest that by selectively altering the absorption characteristics of PMMA, laser removal of bone cement can be achieved. In addition, this study also shows that bone tissue does not absorb visible light energy at 514 nm, suggesting that bone cement may be removed with minimal damage to the surrounding bone tissue. Lasers Surg. Medicine 20:280–289, 1997.

Key words: laser ablation; PMMA; methylene blue; bone cement; revision surgery

INTRODUCTION

Polymethylmethacrylate is a compound used extensively in orthopaedic surgery for the fixation of prosthetic components to bone in total joint arthroplasty. It is estimated that over 120,000 total hip replacements are performed each year in the United States [1]. PMMA has proven to be successful due to its excellent strength and durability, especially in older more sedentary patients [2]. However, studies have shown a high incidence of loosening, notably in younger, more active patients [2,3,4]. Consequently, as an increasing number of younger patients undergo total hip replacements, the number of revision surgeries is likely to increase as well.

Revision of cemented THAs has proven to be more complicated than the initial operation. It is necessary to remove all of the existing cement in order to obtain good fixation between the new implant and bone. However, the mechanical properties of PMMA and its interpenetration into the cancellous bone meshwork make its removal very

Contract grant sponsor: NIH; Contract grant number: AR42395.

*Correspondence to: Cynthia Roberts, Ph.D., Biomedical Engineering Center, The Ohio State University, 270 Bevis Hall, 1080 Carmack Road, Columbus, OH 43210.

Accepted for publication 20 April 1996.

difficult. Current surgical procedures used for removing bone cement are mechanical and require the use of high-speed burrs, reamers, and other instruments that cause bone fractures and perforations and the loss of bone mass. A method to remove bone cement by non-mechanical means would greatly benefit both the surgeon and patient. Attempts have been made to remove bone cement by laser, but with very little success [5–8]. Carbon dioxide lasers have shown promise but are cumbersome due to a lack of fiberoptic compatibility, resulting in the use of a bulky articulating arm [9,10]. In this paper, the authors discuss the use of dyes to selectively alter the ablation characteristics of PMMA in order to enhance cement ablation by a fiber optic compatible Argon ion laser.

MATERIALS AND METHODS

The effects of adding methylene blue and red dye #13 to PMMA bone cement to enhance cement ablation were studied. Three cement groups were investigated (undyed, blue dyed, and red dyed PMMA) while varying power and ablation times. Ablation and thermal damage areas were quantified using image processing techniques. In addition, the ablation-to-damage ratio was defined and computed.

Bone Cement

Cement samples were prepared from commercially available PMMA bone cement [Surgical Simplex P, Howmedica, Rutherford, NJ]. Blue cement samples were made by adding a 1 ml vial of liquid methylene blue dye to each 40 g package of bone cement powder prior to mixing with the monomer solution. Nine samples were prepared and cured in polytetrafluoroethylene cylindrical molds (diameter = 17 mm, height = 30 mm). The red samples were prepared similarly, except with the addition of 0.1 g of red dye #13 powder to each 40 g package of cement powder. Nine red samples were also prepared. Each cement sample was allowed to cure for 1 hr at room temperature. The ends of the cylindrical cement specimens were cut flat with a low speed diamond wheel saw [Model 660, South Bay Technology, Temple City, CA].

Spectroscopy

Cement and bone specimens were cut into thin sections (<50 μm) using a low speed diamond wheel saw. Bone specimens (human tibial cortex) were thawed, sectioned longitudinally, and hand polished on glass with alumina paste until translucent. A spectrophotometer [UV/VIS Lambda 6, Perkin Elmer Corp., Norwalk, CT] measuring wavelengths in the visible light range was used in conjunction with an integrating sphere to determine light transmittance through bone tissue, undyed PMMA, blue dyed PMMA, and red dyed PMMA cements. All specimens were mounted individually on a removable plate that sits inside the spectrophotometer. Transmittance was recorded as a function of wavelength for each sample.

Laser Irradiation

A continuous wave Argon ion laser (λ = 514 nm) [Cooper Lasersonics, Santa Clara, CA] was used for the ablation of bone cement samples. Laser energy was delivered via an optical fiber (fiber diameter = .4 mm) [Cooper Lasersonics, Santa Clara, CA]. Three power levels were selected for ablation (1.5, 2.3, and 3.0 W). At each power setting, an ablation time of 30, 60, 90, or 120 sec was used. A mechanical shutter with adjustable timer was used to control laser energy exposure time [Uniblitz Shutter Driver/Timer, Rochester, NY]. Power settings were confirmed with a power meter [Newport Research, Fountain Valley, CA] before and after ablation.

Consistent placement of the cement sample was achieved by using the fixture shown in Figure 1. The base of the specimen fixture was positioned along the edge of a guide rail. The guide rail was used to provide easy movement of the fixture and power meter while maintaining a constant distance of 3.5 mm between the fiber tip and the cement sample. Each specimen was ablated four times, at 30, 60, 90 and 120 sec (Fig. 2a). A minimum distance of 7 mm was maintained between each irradiated site to ensure that thermal damage zones did not overlap.

A constant spot diameter of 4.5 mm was confirmed using thermal paper and maintained by securely fixing the fiber tip (Fig. 1). Preliminary studies determined that a minimum distance for ablation was needed between the fiber tip and the transverse plane of the cement sample. When the fiber tip was held very close (<2 mm) to the cement surface, ablation did not occur. As laser energy was delivered to the cement, cement vaporization caused minute particles to be ejected into the laser light path, scattering the light and eliminating the ability to ablate PMMA. To remove debris, as well as toxic particles produced during laser ablation of PMMA [7], a vacuum hose was placed near the site of ablation.

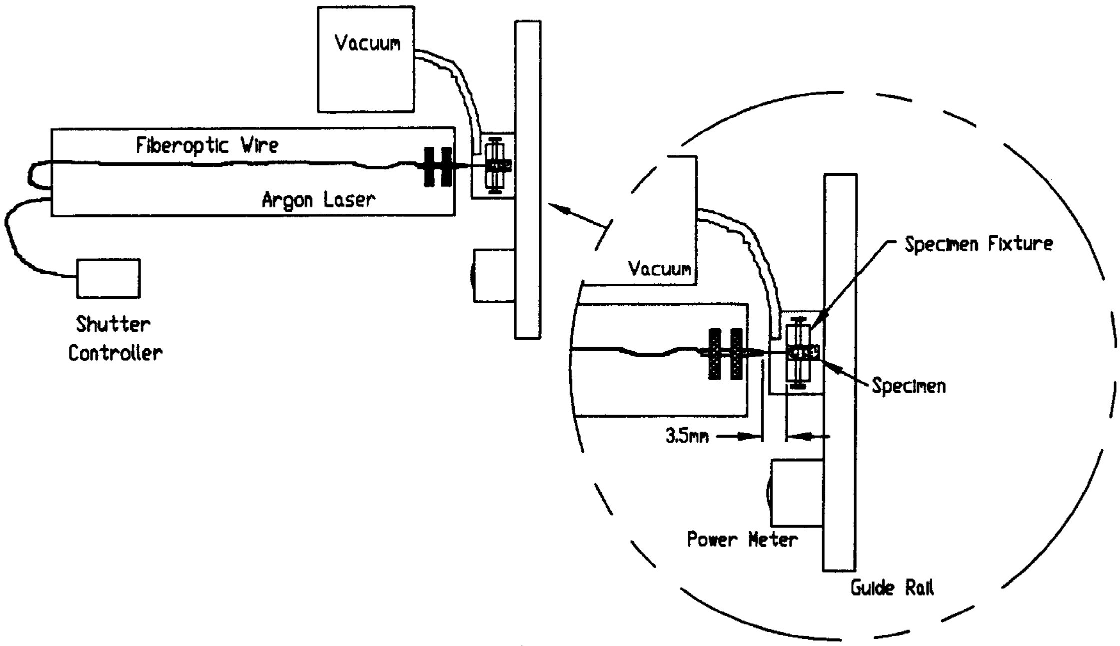

Fig. 1. Experimental setup includes a continuous wave Argon ion laser ($\lambda = 514$ nm) with fiberoptic cable, shutter controller, power meter, vacuum, and specimen fixture. A distance of 3.5 mm was maintained between fiber tip and cement specimen to ensure a constant spot size.

Image Processing

Each ablated cement specimen was sectioned through the center of the ablated area to a thickness of approximately 400 μm with a low speed diamond wheel saw. The specimens were then digitized along with a 1 mm scale at 512 × 512 pixel resolution [Eikonix 78/99 Digital Scanner, Bedford, MA]. All images were manually focused and scanned in full color. Features of the digitized cement sample images were manually traced using a digitizing tablet [Calcomp Digitizing Pad, Anaheim, CA]. The 1 mm scale was used to determine the scale factor for all calculations. An area calculation program was written to evaluate macroscopic changes in the cement in terms of ablation area at the crater center; damage area; and ablation area-to-damage area ratio, as described below.

A digitized image of red PMMA is shown in Figure 2a. The corresponding processed image is shown in Figure 2b. The 1 mm scale shown to the right of the cement specimen was entered by tracing two lines along the width of the scale, as shown. The damage zone was defined as the brightly distinct region of altered cement structure surrounding the ablated area and was outlined by tracing a line that fully enclosed this region. At subthreshold power levels, damage area was present without ablation. At higher power levels, damage area surrounds the ablation zone (Fig. 2b). Points A and B were entered and line AB served as a boundary in the calculation of ablation area. Points A and B lie on the plane of the cement specimen that is perpendicular to the laser delivery axis (Fig. 2b). Ablation area was defined as the area bounded by the intersection of the inner damage area line and line AB. Also, two expanded areas are shown that extend beyond line AB. As laser energy was delivered to the cement, cement temperature rose causing thermal expansion. Temperatures continued to increase until cement vaporization occurred. Consequently, PMMA and the damage zone expand beyond line AB. This expansion area was included in the total damage area calculation. Also, in order to maintain consistency, all images were digitized and traced by one person. The calculation program was verified by digitizing an object with known dimensions. Reproducibility was also verified by digitizing four arbitrary samples three times each producing differences in ablation and damage areas of less than 1%.

Analytical Methods

Ablation and damage areas were determined for each specific power level and ablation time.

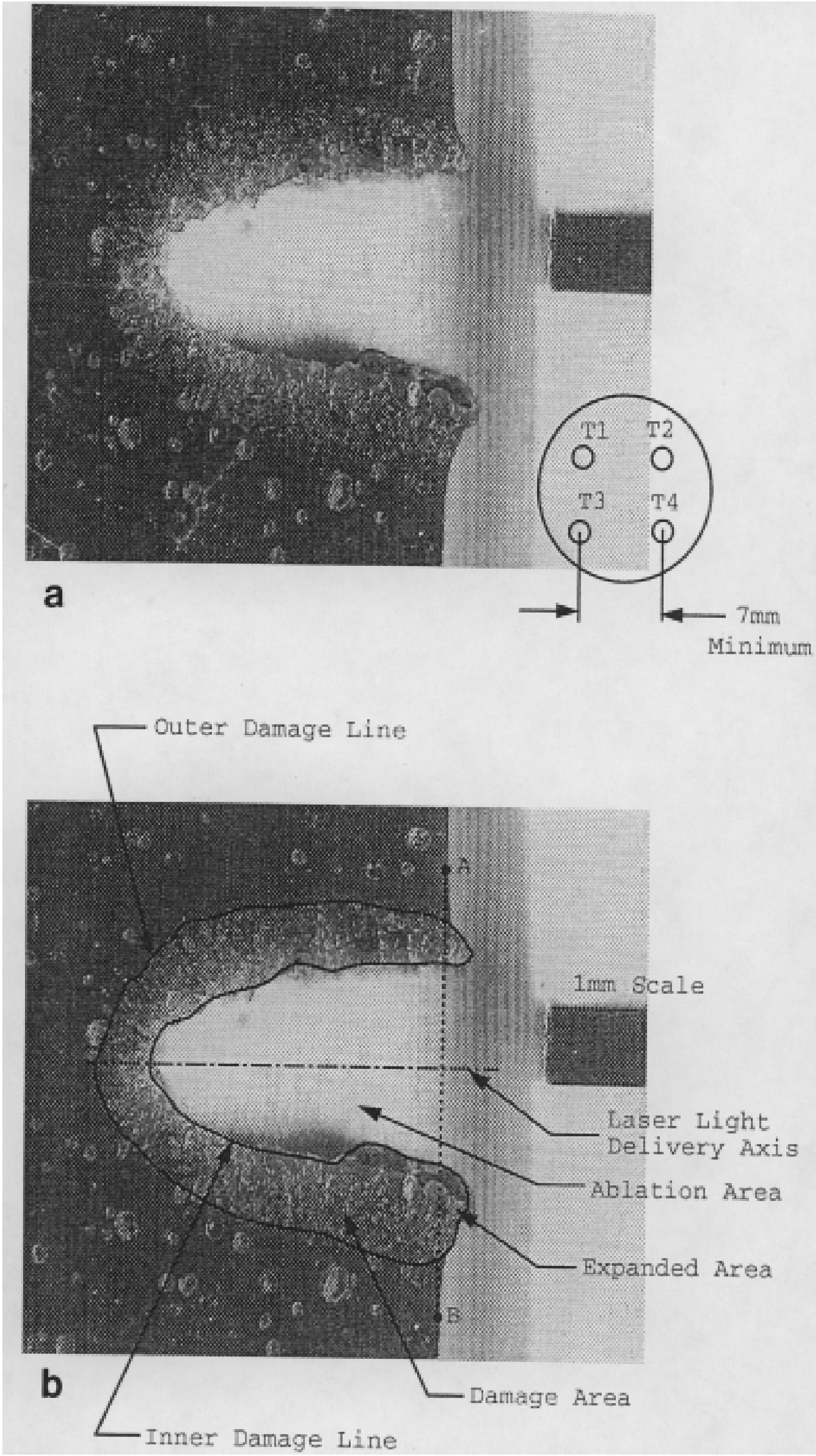

Fig. 2. **a:** Shown is a digitized image of red dyed PMMA cement specimen ablated at 3 W (t = 60 sec) and sectioned through the crater center (parallel to the laser light axis). The brightly discolored region surrounding the ablated area is defined as the damage area. Lower right corner shows pattern for cement ablation where T1 = 30 sec, T2 = 60 sec, T3 = 90 sec, and T4 = 120 sec. A minimum distance of 7 mm was maintained between each irradiated site to prevent overlapping of damage zones. **b:** Shown is a processed image of red dyed PMMA cement specimen ablated at 3 W (t = 60 sec). Damage area was determined by digitizing a line that encloses the entire damage zone (damage area line was labeled as inner damage line and outer damage line for ease of explanation). Ablation area was determined by first digitizing points A and B which lie on the flat end surface of the cement which is perpendicular to the axis of ablation. The area bounded by the intersection of line AB and the inner damage line defines the ablation area. The areas that lie to the right of line AB represent expanded areas caused by thermal expansion during ablation, which was also included in the total damage area calculation. The 1 mm scale was also defined by digitizing two lines along the width of the scale.

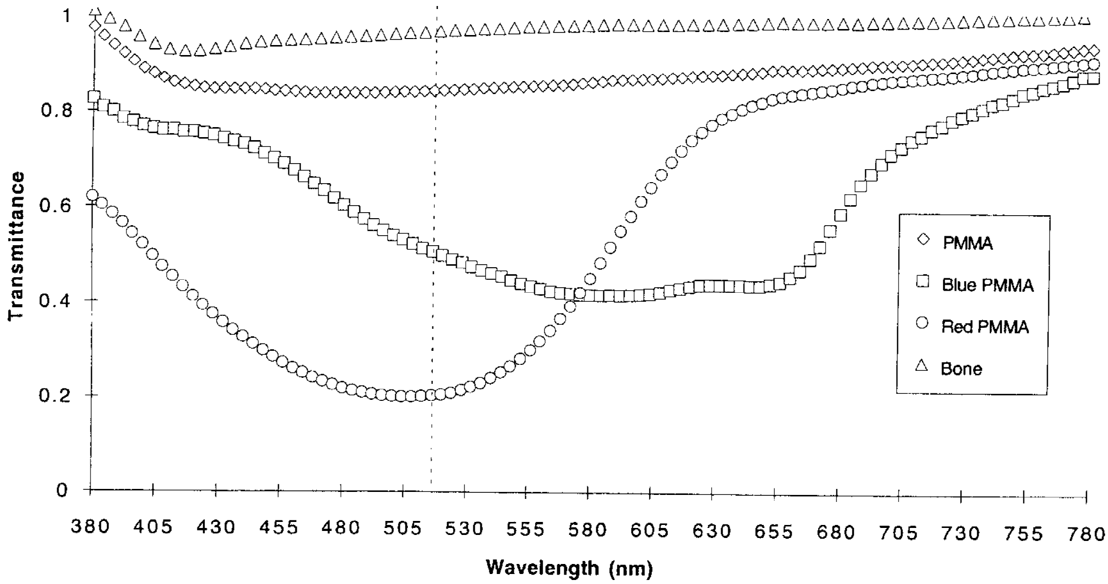

Fig. 3. Transmittance curves for bone, red, blue, and undyed PMMA cement samples in the visible light range. Dotted line indicates $\lambda = 514$ nm, the wavelength of the Argon laser used in the ablation experiments. Red PMMA has significantly greater absorption than blue PMMA at this wavelength. Neither bone nor undyed PMMA has any appreciable absorption at 514 nm.

Areas were calculated by a computer algorithm utilizing a 1 mm scale that was digitized alongside each ablated area. A Student's *t*-test was used to determine statistical significance between mean ablation areas of red PMMA and blue PMMA at each power level and ablation time.

RESULTS

To illustrate the absorption properties of bone tissue, red PMMA, blue PMMA, and undyed PMMA, a transmittance plot within the visible light range is shown in Figure 3. A peak in transmittance indicates low light absorption and vice-versa. The transmittance curve for red PMMA has a distinct minimum near 505 nm, indicating high light absorption in this region. The transmittance curve for blue PMMA shows absorption between 560 to 670 nm. This is consistent with a maximum absorption wavelength of 665 nm for methylene blue dye [11]. The transmittance curves for undyed PMMA and bone show no minimum, indicating very low light absorption across the entire visible range.

The damage and ablation area calculations from cement ablation are shown in Table 1. Mean ablation and mean damage areas were determined from a sample size of $n = 9$ for each cement group. Ablation was not observed for the undyed PMMA cement group, at any of the energy levels tested. However, increases in mean ablation area and damage area for red and blue PMMA cement groups were observed as power and ablation time increased. At a power setting of 1.5 W (at $t = 30$, 60, 90, 120 sec), mean ablation area for red PMMA increased from 0.814 to 3.820 mm^2 while mean damage area increased from 2.201 to 5.362 mm^2. At 2.3 W, mean ablation area increased from 1.896 to 9.037 mm^2 and mean damage area increased from 3.306 to 11.105 mm^2. Increasing the power further to 3.0 W, mean ablation area increased from 5.306 to 14.519 mm^2 and mean damage area increased from 4.991 to 17.976 mm^2.

Increases in ablation area and damage area for blue PMMA cement groups were also observed. At 1.5 W (at $t = 30$, 60, 90, 120 sec), mean ablation area increased from 0.0 to 0.341 mm^2 and mean damage area increased from 1.833 to 2.788 mm^2. At 2.3 W, mean ablation area increased from 0.235 to 3.629 mm^2 and mean damage area increased from 2.770 to 8.803 mm^2. At 3.0 W, mean ablation area increased from 1.688 to 8.686 mm^2 and mean damage area increased from 3.138 to 12.345 mm^2.

The results of mean ablation area in a constant energy comparison (90 and 180 J) are shown in Table 2 and Figure 4. Maximum ablation was achieved at the highest power setting (3 W) for red and blue PMMA. This was apparent in both groups even though the total energy delivered

TABLE 1. Mean Ablation and Damage Area Calculations

Power (W)	Time (sec)	Energy (J)	Fluence J/cm^2	Ablation area red (mm^2) Mean	S.D.	Ablation Area blue (mm^2) Mean	S.D.	Damage area red (mm^2) Mean	S.D.	Damage area blue (mm^2) Mean	S.D.	AblA/DamA red	AblA/DamA blue	P value
1.5	30	45	299.2	0.814	0.173	0.000	0.000	2.201	0.272	1.833	0.337	0.370	0.000	.0001
1.5	60	90	598.5	1.990	0.311	0.000	0.000	3.191	0.410	2.678	0.401	0.624	0.000	.0001
1.5	90	135	897.7	3.070	0.442	0.027	0.047	4.690	0.631	2.555	0.825	0.655	0.011	.0001
1.5	120	180	1197.0	3.820	0.486	0.341	0.326	5.362	0.692	2.788	0.354	0.712	0.122	.0001
2.3	30	69	458.8	1.896	0.563	0.235	0.345	3.306	0.305	2.770	0.458	0.574	0.085	.0001
2.3	60	138	917.7	4.628	0.776	1.519	1.510	5.930	0.632	5.010	1.415	0.780	0.303	.0002
2.3	90	207	1376.5	6.572	0.807	2.473	2.063	8.861	0.798	6.059	2.048	0.742	0.408	.0002
2.3	120	276	1835.4	9.037	1.629	3.629	1.770	11.105	0.751	8.803	1.514	0.814	0.412	.0001
3	30	90	598.5	5.306	1.853	1.688	0.980	4.991	1.240	3.138	0.604	1.063	0.538	.0002
3	60	180	1197.0	9.126	0.771	3.569	1.278	9.076	1.025	5.949	1.013	1.006	0.600	.0001
3	90	270	1795.5	12.158	1.588	6.375	1.900	14.072	1.359	9.113	1.278	0.864	0.700	.0001
3	120	360	2393.9	14.519	1.295	8.686	2.488	17.976	1.697	12.345	2.394	0.808	0.704	.0001

was constant. At 90 J, ablation of red PMMA was 2.7 times greater at 3.0 W (t = 30 sec) than at 1.5 W (t = 60 sec). At 180 J, ablation was 2.4 times greater at 3.0 W (t = 60 sec) than at 1.5 W (t = 120 sec). The difference in ablation area for blue PMMA was more significant at the higher power setting. At 90 J, ablation at 1.5 W (t = 60 sec) was not possible (subthreshold). However, at 3.0 W (t = 30 sec) the mean ablation area was 1.688 mm^2. At 180 J, ablation was 10.5 times greater at 3.0 W (t = 60 sec) than at 1.5 W (t = 120 sec).

Similar results were also seen with maximum damage area occurring at the highest power setting (Fig. 5, Table 2). At 90 J, the damage area of red PMMA was 1.6 times greater at 3.0 W (t = 30 sec) than at 1.5 W (t = 60 sec). At 180 J, damage area was 1.7 times greater at 3.0 W (t = 60 sec) than at 1.5 W (t = 120 sec). The difference in damage area for blue PMMA at 90 J was 1.2 times greater at 3.0 W (t = 30 sec) than at 1.5 W (t = 60 sec). At 180 J, damage area was 2.1 times greater at 3.0 W (t = 60 sec) than at 1.5 W (t = 120 sec).

A two sample t-test was used to determine statistical significance between mean ablation areas and mean damage areas of the same energy level. Statistical results indicate significant differences at 90 and 180 J for red and blue ablation areas with $P < .001$ (Table 2). Statistical differences also exist for red and blue damage areas at 90 and 180 J with $P < .003$, except for mean damage areas of blue PMMA at 90 J. The blue cement samples irradiated at 90 J did not show a significant difference between damage areas with $P = .19$ (Table 2).

The mean ablation-to-damage ratio calculations for red and blue PMMA are also shown (Table 1). Results indicate that increasing energy produced increasing ablation-to-damage ratios, with exception to the red PMMA cement group ablated at 3.0 W.

Statistical significance between red and blue ablation areas were also determined using a two sample Student's t-test (Table 1). All P values ($P < .0002$) indicate strong statistical differences between red and blue mean ablation areas, with greater ablation occurring in red PMMA cement.

DISCUSSION

The ability to remove bone cement without damaging surrounding bone tissue during revision joint surgery is not possible with current surgical techniques. Numerous alternative procedures have been investigated [12–16]. The carbon dioxide laser has shown promise in removing bone cement [9,10]. However, since the CO_2 laser emits energy in the far infrared range of the electromagnetic spectrum, fiber optic delivery is not possible. As a result, optical lenses and mirrors are necessary in order to deliver laser energy, resulting in a bulky articulating arm which makes its use somewhat cumbersome. This delivery system also makes the removal of bone cement in the distal regions of the femur very difficult. In addition, studies have shown that CO_2 lasers have the ability to cut and thermally damage bone tissue [17,18]. An alternative device that can efficiently remove bone cement with minimal damage to the surrounding bone tissue is desirable.

In this study, the Argon laser was unsuccessful in ablating standard commercially available PMMA bone cement at any of the energy levels tested. In order to have radiant energy absorbed, it is necessary to have absorbing molecules or

TABLE 2. Constant Energy Analysis

Power (W)	Time (sec)	Energy (J)	Mean ablation area Red (mm^2)	Mean ablation area blue (mm^2)	Mean damage area red (mm^2)	Mean damage area blue (mm^2)
1.5	60	90	1.990	0.000	3.191	2.678
3	30	90	5.306	1.688	4.991	3.138
			(P = .0001)	(P = .0010)	(P = .0026)	(P = .1900)
1.5	120	180	3.820	0.341	5.362	2.788
3	60	180	9.126	3.569	9.076	5.949
			(P = .0001)	(P = .0007)	(P = .0001)	(P = .0001)

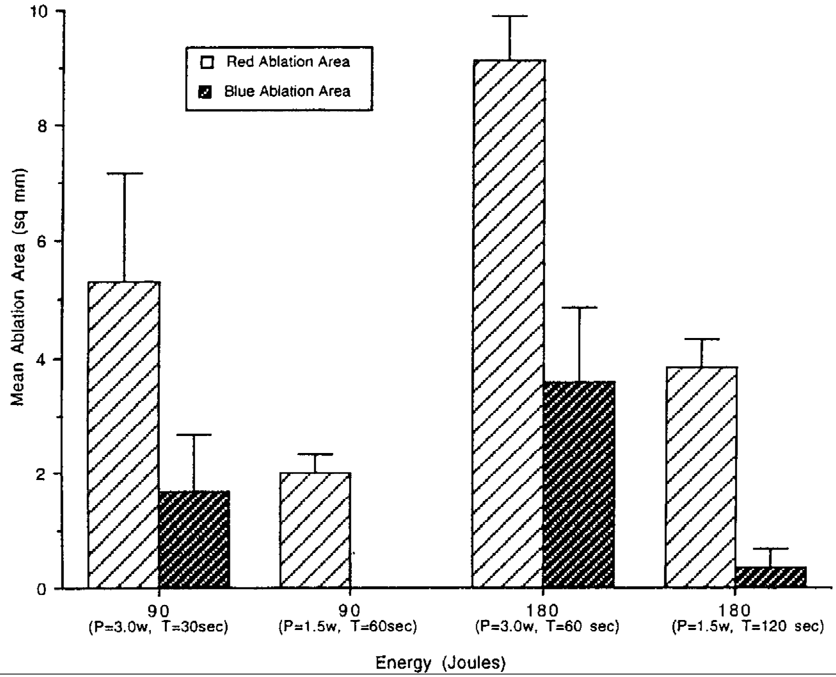

Fig. 4. Shown are mean ablation areas for red and blue PMMA as a function of constant energy (90 and 180 J). The graph shows significant differences in ablation areas for both cement groups, even when energy delivered was held constant. Greater ablation was achieved when ablated at 3.0 W for both cement groups. This suggests that ablation at lower power levels with longer ablation times is not as efficient as ablation at higher power levels with shorter ablation times.

chromophores in the target tissue. Visible spectrophotometry of undyed PMMA shows the absence of an absorption peak near 514 nm, the output wavelength of the Argon laser (Fig. 3). The lack of an absorption peak explains why the Argon laser will not ablate undyed PMMA. This is consistent with other studies that were also unable to efficiently ablate bone cement at wavelengths not coinciding with the absorption wavelengths of PMMA [5,6,19]. The absorption characteristics of PMMA can be altered by the addition of either methylene blue or red dye #13, two visible light absorbing agents. Visible spectrophotometry shows absorption between 560 and 670 nm for blue PMMA and a very strong absorption peak near 505 nm for red PMMA. This suggests that for energy delivered at a wavelength of 514 nm, red PMMA will have greater absorption than blue PMMA cement.

The selection of methylene blue and red dye #13 was based on several criteria: solubility in bone cement, thermal stability during cement polymerization, availability, and the presence of absorption peaks within the visible light range. The latter criterion is important since the Argon laser selected delivers energy at 514 nm, also within the visible light range. However, other issues that also need to be considered include biocompatibility and long-term leaching effects of both dyes. The use of methylene blue dye in medical applications is not new. Methylene blue dye has been used as a diagnostic agent, an antimethemoglobinemic agent, and for the differential cytophysical diagnosis of cancerous and normal tissues

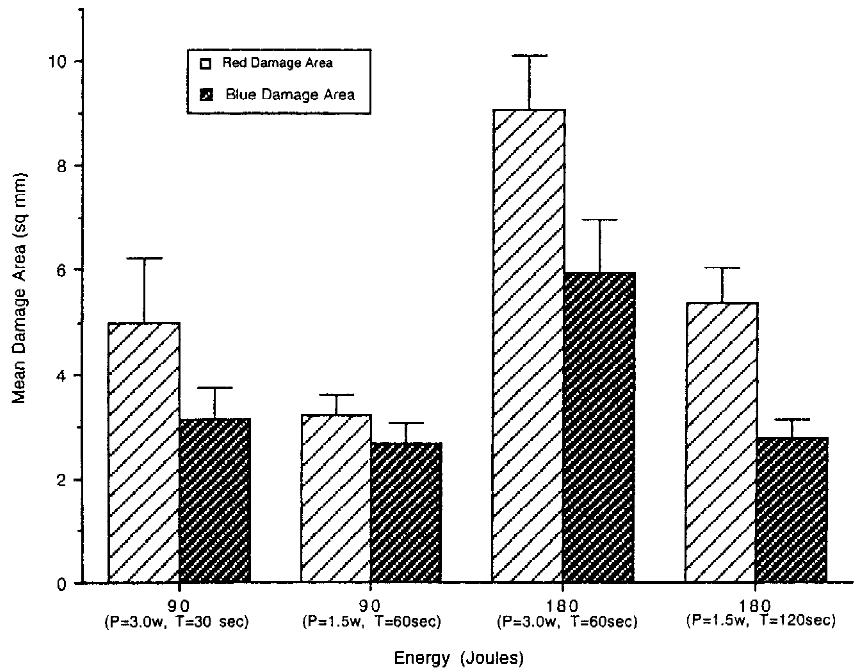

Fig. 5. Shown are mean damage areas for red and blue PMMA as a function of constant energy (90 and 180 J). The graph shows significant differences in damage areas for both cement groups except for the blue cement group ablated at 90 J. Greater damage area was produced when ablated at higher power levels with shorter exposure times vs. at lower power levels with longer exposure times.

[20]. On the other hand, red dye #13 is not approved for medical use. Red dye #13 is for experimental use only, due to its high toxicity. However, red dye #13 was selected due to its absorption peak near the 514 nm wavelength of the Argon laser. The long-term issue of leaching is also very important and will be discussed briefly at this time. Both dyes showed considerable leaching when lubricated with cutting solution in the low speed saw during specimen preparation. However, it is not certain whether the dyes were released due to the cutting action of the saw or just by passively leaching out of the cement. Nevertheless, the use of dyes in PMMA for dental applications is very common and leaching is not a problem due to proprietary manufacturing techniques. This suggests that the problem of methylene blue dye or any other biocompatible dye leaching from bone cement can be similarly solved.

The evaluation of the areas calculated from image processing indicates that as laser energy increases, damage area and ablation area increase in both blue and red PMMA cement (Table 1). More importantly, at each power level tested, the mean ablation areas of red PMMA were all significantly greater than the mean ablation areas of blue PMMA. This verified the expectation that since the absorption peak of red PMMA is much closer to the output wavelength of the Argon laser (Fig. 3), more energy was absorbed resulting in increased cement ablation. Statistical significance was shown with all P values less than .0002 (Table 1). The damage areas for red and blue PMMA also showed that increasing energy produced increasing damage area. The maximum damage area for both groups occurred when cement was ablated at 3 W, even when energy was held constant (Fig. 5). Furthermore, constant energy comparisons suggest that varying power and ablation time produces significantly different amounts of ablation and damage area. Table 2 shows that at twice the power level (3.0 vs. 1.5 W), but at half the exposure time (30 vs. 60 sec), the ablation areas for red and blue PMMA were significantly greater. It is possible that low powered lasers ablating at longer ablation times may not be able to efficiently remove PMMA even if the laser's output wavelength matches that of the cement. Nonetheless, the combination of power and ablation times used in this study produced damage areas that are far too large relative to the ablation areas. A possible solution to reduce damage area is to use a pulsed laser. A pulsed laser

would allow thermal energy to dissipate between pulses thereby minimizing the damage zone.

The analysis of the ablation-to-damage ratio suggests that the optimal parameters for ablating red PMMA in this study occur at a power setting of 3.0 W (30 sec, 90 J) (Table 1). This corresponds to a maximum mean ablation-to-damage ratio of 1.063, indicating that more cement was removed than damaged. Further increases in energy, by increasing ablation time, only produced lower ablation-to-damage ratios (i.e., greater damage area than ablation area). In comparison, the ablation-to-damage ratio for blue PMMA also increased at each power setting. However, a peak was not reached indicating that the optimal ablation parameters for blue PMMA were not achieved from the parameters selected in this study. Therefore, an increase in power is possible. However, proportional increases in damage area will also result. Additionally, ablation area of blue PMMA did not occur until ablation time was increased to 90 sec (1.5 W, 135 J). Energy below this level (1.5 W) was likely subthreshold for the ablation of blue PMMA.

The results of this study suggest that it is possible to alter the absorption characteristics of standard PMMA to enhance cement ablation by an Argon ion laser. The ability to selectively alter the absorption characteristics of PMMA is very important. One of the significant disadvantages of the CO_2 laser is its ability to thermally damage bone. The use of dyes to alter the absorption wavelength of PMMA allows for the absorption of laser energy at a wavelength that is not absorbed by bone tissue. The transmittance plot indicates that bone does not absorb light energy in the visible range of the EM spectrum (Fig. 3). Since methylene blue dye is approved for clinical use and is distinguishable in blood, it is a good candidate to be used with commercially available bone cement. Another advantage is that a fiberoptic compatible laser can now be utilized. The ability to deliver energy through a fiber provides flexibility not available from the CO_2 laser. In future studies, a tunable dye laser with visible output wavelengths could be used to better match the absorption wavelength of methylene blue dye to further enhance cement ablation. Also, the use of a pulsed laser should be considered to minimize the amount of thermal damage produced during ablation. Finally, the long-term leaching effects of dyes must be addressed as well as the ablation of PMMA at the cement-bone interface to determine the effects of visible light energy on bone viability.

ACKNOWLEDGMENTS

This study was partially supported by NIH grant AR42395. The authors thank Howmedica for supplying Simplex P bone cement for use in this study and the Vascular Diseases Lab in the Biomedical Engineering Center at Ohio State University, especially Ed Herderick, for assistance with the image processing.

REFERENCES

1. NIH Consensus Statement. Total hip replacement. National Institute of Health. September 1994, vol 12, no 5.
2. Holman PR, Tyer HD. Porous coated anatomic non-cemented total hip arthroplasty. Aust N Z J Surg 1992;62:56.
3. Amstutz, HC, Nasser S, More RC, Kabo JM. The anthropometric total hip femoral prosthesis: Preliminary clinical and roentgenographic findings of exact-fit cementless application. Clin Orthop 1989;242:104.
4. Chandler HP, Reineck FT, Wixson RL. A five year review of total hip replacements in patients under the age of 30—with emphasis on loosening. Orthop Trans 1979;3:303.
5. Garino JP, Nazarian D, Froimson MI, Grelsamer RP, Treat M. A comparison of ablation of polymethylmethacrylate by two fiberoptic compatible infrared lasers. Lasers Orthop Dental Vet Med 1991;SPIE vol 1424:43–45.
6. Nelson SJ, Yow L, Liaw LH, Lachlan M, Zavar RB, Orenstein A, Wright WH, Andrews JJ, Berns MW. Ablation of bone and methacrylate by a prototype mid-infrared erbium:YAG laser. Lasers Surg Med 1988;8:494–500.
7. Choy DS, Kaminow IP, Kaplan M, Case RB, Zickel R. Experimental Nd:YAG laser disintegration of methylmethacrylate. Clin Orthop Rel Res 1985;287–288.
8. Zimmer M, Klobl R, Klobl R, DeToma G, Jansson V, Refior HJ, Heimkes B, Kuhne JH. Bone cement removal with the excimer laser in revision arthroplasty. Arch Orthop Trauma Surg 1992;112:15–17.
9. Booth RE, Gordon SL, Carney MD. Use of the CO_2 laser in revision hip surgery. Contemp Orthop 1987;15:17–22.
10. Sazy J, Kollmer C, Uppal G, Lane G, Sherk H. Endoscopic removal of PMMA in hip revision surgery with a CO_2 laser. Lasers Orthop Dental Vet Med 1991;SPIE vol 1424:50–51.
11. “Catalog Handbook of Fine Chemicals.” Milwaukee, WI: Aldrich, 1994–1995.
12. Caillouette JT, Gorab RS, Klapper RC, Anzel SH. Revision arthroplasty facilitated by ultrasonic tool cement removal. Orthop Rev 1991;4:353–357.
13. May TC, Krause WR, Preslar AJ. Use of high-energy shock waves for bone cement removal. J Arthroplasty 1990;5:19–27.
14. Weinstein JN, Oster DM, Park JB, Park SH, Loening S. The effect of the extracorporeal shock wave lithotriptor on the bone-cement interface in dogs. Clin Orthop Rel Res 1988;235:261–267.
15. Nelson CL, Barnes CL. Removal of bone cement from the femoral shaft using a femoral windowing device. J Arthroplasty 1990;5:67–69.

16. Pierson JL, Jasty M, Harris WH. Techniques of extraction of well-fixed cemented and cementless implants in revision total hip arthroplasty. Orthop Rev 1993;8:904–916.
17. Small IA, Osborn TP, Fuller T, Hussain M, Kobernick S. Observations of carbon dioxide laser and bone burr in the osteotomy of rabbit tibia. J Oral Surg 1979;37:159.
18. Tauber C, Farine I, Horoszowski H. Fracture healing in rabbits after osteotomy—the CO_2 laser. Acta Orthop Scand 1979;50:385–390.
19. Nelson SJ, Yow L, Bernes MW. Ablation of bone and polymethylmethacrylate by an XeCL 308 nm laser. Laser Surg Med 1989;141–147.
20. Gurr E. "Synthetic Dyes in Biology, Medicine and Chemistry." New York: Academic Press, 1971, pp 76, 147.